Carbon nanotubes-enhanced nanocomposite organohydrogel based on a physically cross-linked double network for sensitive wearable sensors

Yexiong Huang,[a,b] Jiabing Yu,[b] Ku Shu [b] and Xianping Chen *[b]

[a] School of Physics and Electronic Engineering, Chongqing Normal University, Chongqing 401331, China.
[b] Department of Optoelectronic Engineering, Key Laboratory of Optoelectronic Technology & Systems, Education Ministry of China, Chongqing University, Chongqing, 400044 China.
[*] Corresponding author. E-mail address: xianpingchen@cqu.edu.cn (Xianping Chen)

Table S1. Compositions for the hydrogel.

Samples	AAm (mg)	SA (mg)	CNTs (mg)	SDS (mg)	LMA (uL)	APS (mg)	TMEDA (uL)	$CaCl_2$ (mg)	NaCl (mg)	Glycerol (mL)	Water (mL)
HPAAm/SA	4.97	0.35	0	0.1	92	18.9	40	0.882	2.6	0	30
HPAAm-CNTs/SA	4.97	0.35	0.1	0.1	92	18.9	40	0.882	2.6	0	30
NOH	4.97	0.35	0.1	0.1	92	18.9	40	0.882	2.6	20	10

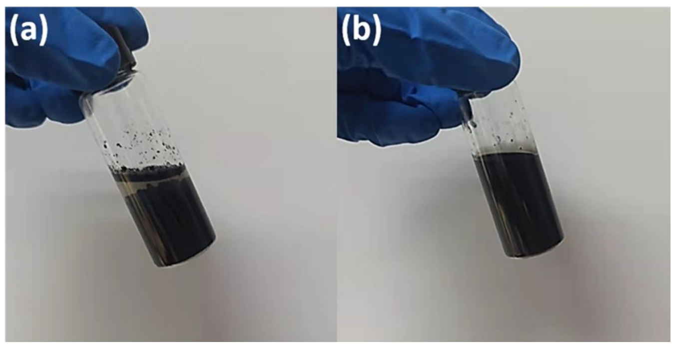

Fig. S1. The photos of the distribution of CNTs in (a) LMA/water, and (b) SDS/LMA solution, respectively. CNTS is easy to aggregate and delaminate in the solution without SDS. It can maintain uniform distribution in the SDS/LMA solution without any aggregation after even 24 h.

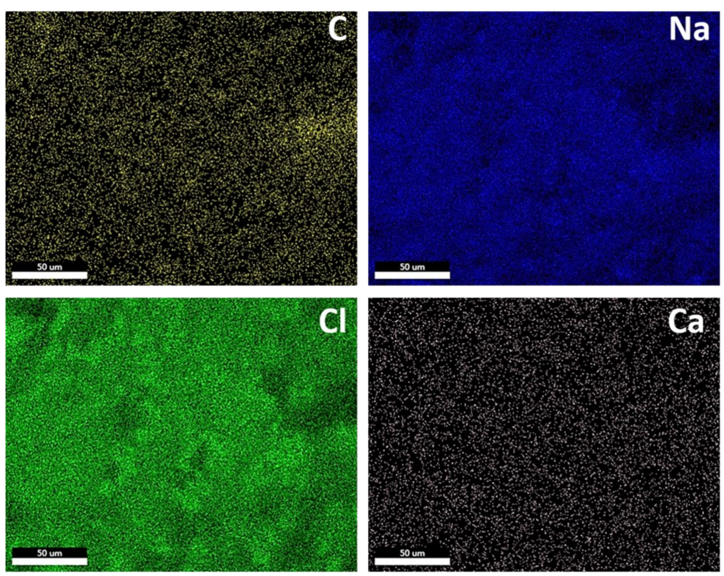

Fig. S2. The distribution of C, Na, Cl, and Ca element in the energy-dispersive X-ray spectroscopy (EDS) mapping.

Table S2. Atomic percentage of the elements.

Element	Atomic %
C	55.03
Na	23.70
Ca	0.31
Cl	20.96

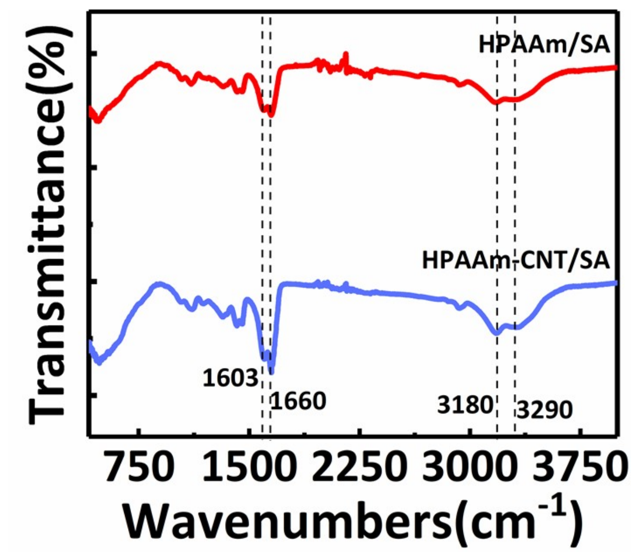

Fig. S3. FTIR spectra of HPAAm/SA and HPAAm-CNT/SA hydrogel.

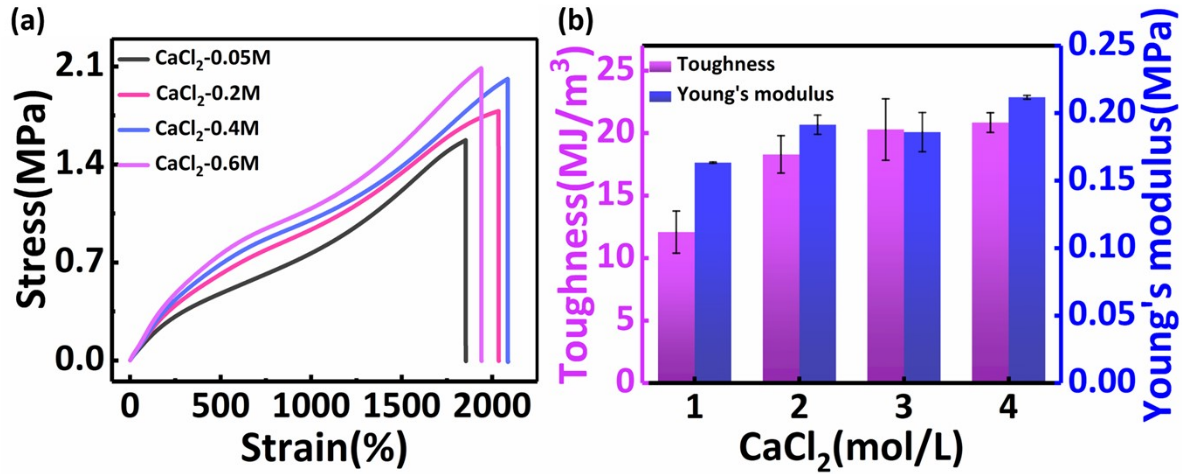

Fig. S4. Tensile stress-strain curves and the corresponding toughness and Young's modulus values of the nanocomposite organohydrogel soaking in the glycerol/water solution (20:10) with different $CaCl_2$ contents.

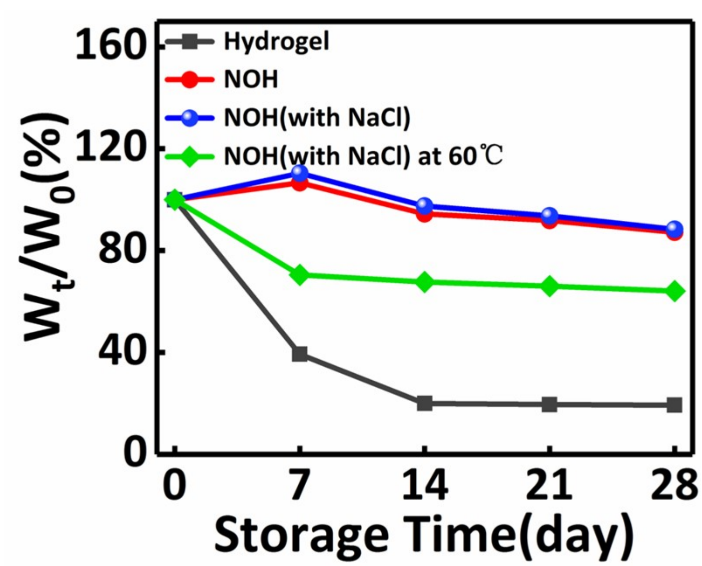

Fig. S5. Weight remaining curves of the samples were stored at room temperature and 60 ℃ for one month. The weight of the hydrogel decreases to the lowest value (about 20% of its initial weight) after being stored at room temperature for two weeks. In contrast, the weight of NOH at room conditions decreases slowly and still maintains 88% of its initial weight after one month. For NOH put under 60 ℃, the weight decreases quickly in the first week and then decreases slowly to about 64% of its initial weight after one month.

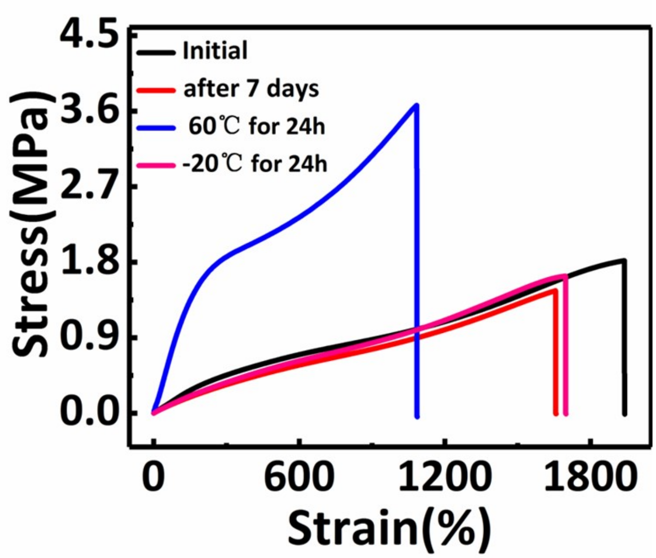

Fig. S6. Tensile stress-strain curves for NOH are stored in different environments.

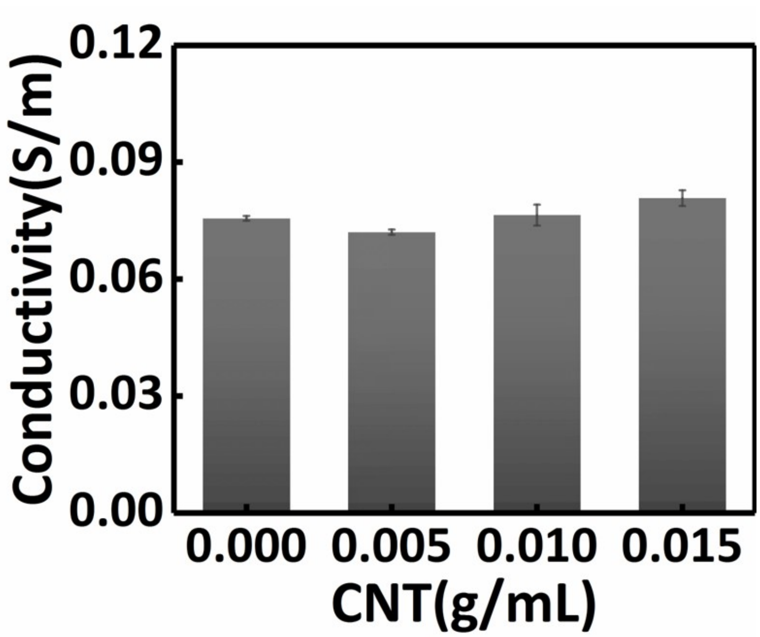

Fig. S7. Conductivity variation with different concentrations of CNTs. (glycerol/water=20:10, $CaCl_2$=0.2 M, NaCl=0 M)

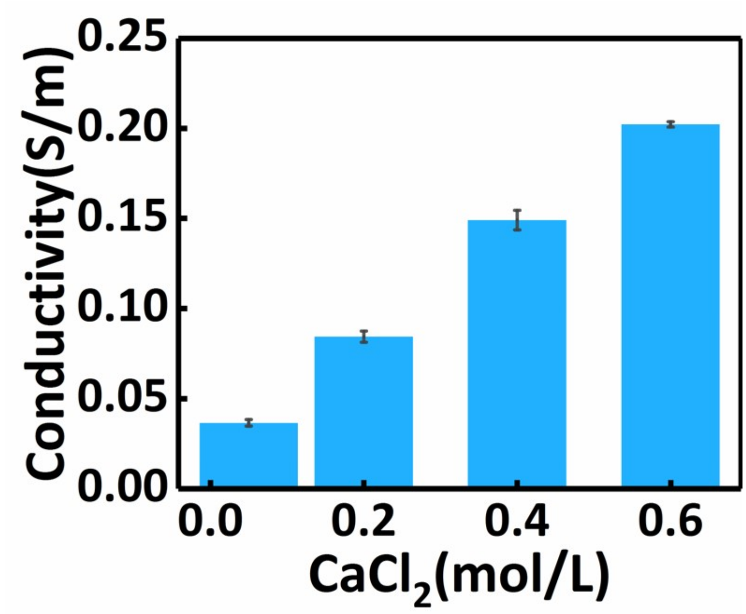

Fig. S8. Conductivity variation with different concentrations of $CaCl_2$ in the solution of glycerol/water(20:10).

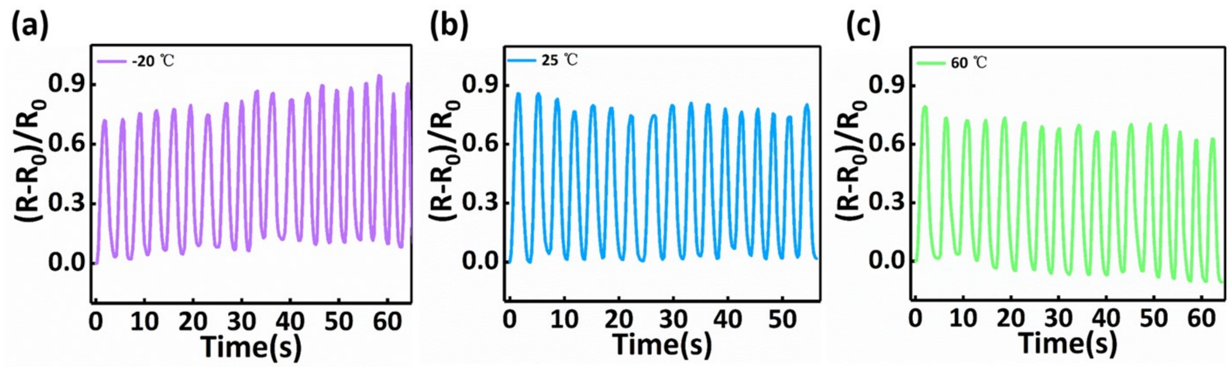

Fig. S9. Relative resistance changes for continuous bending of the finger under (a) -20 ℃, (b) 25 ℃, and (c) 60 ℃, respectively.

Table S3. Comparison of important performances of the prepared nanocomposite organohydrogel and the previous works.

Materials	Stress (MPa)	Strain	Toughness (MJ/m^3)	Anti-freezing agents	Conductivity (S/m)	GF	Ref.
HPAAm/CS-c-MWCNT	0.065	2761%	-	-	0.82	1.65 (0-100%)	1
HAPAA/PANI	0.9	2590%	7.85	-	3.35	2.6 (0-300%)	2
HAPAM/CNC@CNT	0.25	2900%	3.6	-	0.826	1.65 (0-600%)	3
PVA /MXene	0.0054	1200%	-	-	-	0.4 (0-200%)	4
CNTs/HAPAAm	0.267	3000%	3.42	-	1.75×10^{-2}	2.0 (0-300%)	5
PAA-LM/rGO	0.1	2900%	-	-	-	1.77 (0-100%)	6
PAAm-oxCNTs	0.71	1000%	2.29	-	6.7×10^{-2}	1.5 (0-200%)	7
PAM/gelatin/PEDOT: PSS	0.29	2850%	-	-	-	0.46% (0-200%)	8
PAAm-TA@CNF-MXene	0.16	1500%	-	glycerol	0.19	4.15 (0-250%)	9
TA@HAP NWs-PVA	0.36	480%	0.94	glycerol	-	2.84 (0-350%)	10
PVA/Gly/CB/CNT	4.84	640%	15.93	glycerol	0.17	2.01 (0-700%)	11
PVA/PAAm/MXene	0.035	1000%	-	ethylene glycol	1.5×10^{-2}	5.02 (0-200%)	12
PAAM/PVP/Graphene	0.072	21 000%	-	ethylene glycol	-	2.3	13
PAM/MMT/CNTs	0.2	4196%	-	glycerol	$<1.0\times10^{-3}$	2.77 (0-1000%)	14
Alg-PBA/ PVA/PAM/rGO	0.064	610%	-	ethylene glycol	1.1×10^{-2}	$0.0112 kPa^{-1}$	15
PAA/CS/GO	0.226	1000%	1.12	glycerol	6.7×10^{-2}	1.138 (0-80%)	16
HPAAm-CNTs/SA	1.56	1871%	18.3	glycerol	0.48	2.85 (0-200%)	**This work**

1 S. Xia, S. Song, F. Jia and G. Gao, *J. Mater. Chem. B*, 2019, **7**, 4638-4648.
2 G. Su, S. Yin, Y. Guo, F. Zhao, Q. Guo, X. Zhang, T. Zhou and G. Yu, *Mater. Horiz.*, 2021, **8**, 1795-1804.
3 G. Su, J. Cao, X. Zhang, Y. Zhang, S. Yin, L. Jia, Q. Guo, X. Zhang, J. Zhang and T. Zhou, *J. Mater. Chem. A*, 2020, **8**, 2074-2082.
4 J. Zhang, L. Wan, Y. Gao, X. Fang, T. Lu, L. Pan and F. Xuan, *Adv. Electron. Mater.*, 2019, **5**, 1900285.
5 Z. Qin, X. Sun, Q. Yu, H. Zhang, X. Wu, M. Yao, W. Liu, F. Yao and J. Li, *ACS Appl. Mater. Interfaces*, 2020, **12**, 4944-4953.
6 Z. Zhang, L. Tang, C. Chen, H. Yu, H. Bai, L. Wang, M. Qin, Y. Feng and W. Feng, *J. Mater. Chem. A*, 2021, **9**, 875-883.
7 X. Sun, Z. Qin, L. Ye, H. Zhang, Q. Yu, X. Wu, J. Li and F. Yao, *Chem. Eng. J.*, 2020, **382**, 122832.
8 H. Sun, Y. Zhao, C. Wang, K. Zhou, C. Yan, G. Zheng, J. Huang, K. Dai, C. Liu and C. Shen, *Nano Energy*, 2020, **76**, 105035.
9 Y. Wei, L. Xiang, H. Ou, F. Li, Y. Zhang, Y. Qian, L. Hao, J. Diao, M. Zhang, P. Zhu, Y. Liu, Y. Kuang and G. Chen, *Adv. Funct. Mater.*, 2020, **30**, 2005135.
10 J. Wen, J. Tang, H. Ning, N. Hu, Y. Zhu, Y. Gong, C. Xu, Q. Zhao, X. Jiang, X. Hu, L. Lei, D. Wu and T. Huang, *Adv. Funct. Mater.*, 2021, 2011176.
11 J. Gu, J. Huang, G. Chen, L. Hou, J. Zhang, X. Zhang, X. Yang, L. Guan, X. Jiang and H. Liu, *ACS Appl. Mater. Interfaces*, 2020, **12**, 40815-40827.
12 H. Liao, X. Guo, P. Wan and G. Yu, *Adv. Funct. Mater.*, 2019, **29**, 1904507.
13 H. Zhang, W. Niu and S. Zhang, *ACS Appl. Mater. Interfaces*, 2018, **10**, 32640-32648.
14 H. Sun, Y. Zhao, S. Jiao, C. Wang, Y. Jia, K. Dai, G. Zheng, C. Liu, P. Wan and C. Shen, *Adv. Funct. Mater.*, 2021, 2101696.

15 D. Ma, X. Wu, Y. Wang, H. Liao, P. Wan and L. Zhang, *ACS Appl. Mater. Interfaces*, 2019, **11**, 41701-41709.
16 S. Xia, S. Song, Y. Li and G. Gao, *J. Mater. Chem. C*, 2019, **7**, 11303-11314.